Archaeometry **49**, 1 (2007) 153–177. Printed in Singapore

A NEW DATING METHOD FOR HIGH-CALCIUM ARCHAEOLOGICAL GLASSES BASED UPON SURFACE-WATER DIFFUSION: PRELIMINARY CALIBRATIONS AND PROCEDURES*

C. M. STEVENSON

Virginia Department of Historic Resources, 2801 Kensington Avenue, Richmond, Virginia 23221, USA

D. WHEELER

The Thomas Jefferson Foundation, Charlottesville, Virginia 22902, USA

S. W. NOVAK

Evans East, 104 Windsor Center, Suite 101, East Windsor, New Jersey 08520, USA

R. J. SPEAKMAN

Museum Conservation Institute, Smithsonian Institution, Suitland, Maryland 20746, USA

and M. D. GLASCOCK

Research Reactor Center, University of Missouri, Columbia, Missouri 65211, USA

The first European settlers came to North America in the early 17th century using glass in the form of containers and decorative objects. Thus, glass is a horizon marker for all historic period settlements and a potential source of chronometric dates at archaeological sites belonging to the historic period in the Americas. We have developed a new absolute dating method based upon water diffusion into the surface of manufactured glasses that predicts diffusion coefficients based upon variation in glass chemical constituents. Low-temperature (< 190°C) hydration experiments have been performed on a set of five high-calcium (21.7–28.3%) glasses that were used to manufacture wine bottles from the 17th–19th centuries. Infrared spectroscopy and secondary ion mass spectrometry was used to model the water diffusion/alkali exchange process. The ability of the model to accurately predict archaeological ages was evaluated with artefacts recovered from ceramic-dated contexts at Thomas Jefferson's plantation known as Monticello.

KEYWORDS: ALKALI EXCHANGE, DATING, DIFFUSION, GLASS, INFRARED, MEAN CERAMIC DATE, MONTICELLO, SIMS, VAPOUR HYDRATION

INTRODUCTION

The dating of manufactured glasses from historical archaeological contexts, based upon the amount of surface-diffused ambient water, is a new chronometric tool that can be used to structure interpretations of the recent past. The normal high frequency of glass shards at historic

*Received 3 October 2005; accepted 15 March 2006

North American period sites starts with 17th century Colonial occupations and continues to the present. As a result, there is no lack of potentially datable material available to the archaeologist. Such an approach becomes feasible when the diffusion of water into a glass surface becomes predictable at a high level of accuracy. In this paper, we present new experimental calibrations that allow the age estimation of high-calcium (21.7–28.3%) glasses recovered from archaeological contexts. The capability of the calibrations to estimate the correct age is tested with artefacts recovered from an independently dated context in Building o at Thomas Jefferson's Monticello Plantation in central Virginia.

Historical archaeological contexts can be dated by a number of approaches that include kaolin pipe stem bore diameters (Binford 1962; Heighton and Deagan 1971; Deetz 1987), wine bottle morphology (Noel Hume 1970), ceramic forms and decorative elements (Wilcoxen 1987; Miller 2000) and ceramic makers' marks (Kovel and Kovel 1953, 1986). All of these methods provide chronological information about the period of manufacture that may last years or decades in duration. As such, in many cases the dating of manufactured items provides only a general guide to age. These estimates can at times be influenced significantly by the long-term curation of cultural material before it enters the archaeological record (Adams 2003). Therefore, the most useful dating methods are the ones where the time between the cultural event, and the material used to date the event, is minimized (Dean 1978). For example, it is preferable to radiocarbon date a hearth fire with annual plants rather than the limb of an old tree. In the glass dating procedures developed here, we target the fracture surface of bottle fragments under the assumption that glass shards enter the archaeological record soon after bottle breakage.

WATER DIFFUSION IN GLASS

Lanford (1977, 1978) was the first researcher to propose the idea of monitoring water diffusion into the surface of manufactured glasses as the foundation of a dating method. He used ^{15}N resonance profiling of the glass surface to develop a series of hydrogen profiles that represented the depth of water diffusion over time at a constant temperature. These experiments demonstrated that water diffused into the surface of glass in a regular manner, where depth of diffusion increased according to the square root of time. Further investigations from an archaeological dating perspective were not continued, and we are not aware of any applications of glass hydration dating to historical glass artefacts.

A considerable number of investigations have looked at the basic process of hydration in simple soda–lime–silicate glasses. Doremus (1975) originally proposed that hydronium ions (H_3O^+) enter the glass surface and react with the glass network, with the consequence that the structure becomes increasingly open as the glass deteriorates. Subsequent to this, diffused molecular water enters the open network and further reacts with the silica–oxygen structure, replacing sodium ions that migrate to the glass surface/water interface. This process leads to further hydration and eventual dissolution of the glass matrix. The model specifying that H_3O^+ was the mobile water species was supported by the observation that the ratio of sodium to diffused hydrogen was approximately 1:3 (Lanford 1977; Romich 2003), meaning that three hydrogen atoms replaced a single sodium atom.

While this basic exchange process has remained accepted until the present, another exchange mechanism has been proposed by Smets and Lommen (1983), who argued that H_2O is responsible for glass leaching under near-neutral conditions in the pH range of 4–7:

$$= SiO^-Na^+ + H_2O > > > SiOH + Na^+OH^-$$

In this model, molecular water enters the glass network, disassociates and bonds with non-bridging oxygen sites to form silanol groups. As a result of charge compensation, the sodium ions become mobile and migrate to the surface of the glass along with hydroxyl co-ions (OH^-). In this model, there is a one-to-one replacement of sodium with hydrogen atoms. However, the ratio of the two can be greater than one as a result of subsequent water diffusion as the glass structure becomes less rigid.

In the model by Smets and Lommen (1983), the exchange process for molecular water is determined by the number of available non-bridging oxygen sites (NBOs). Increasing the proportion of sodium to silica, for example, would accelerate the rate of molecular water diffusion. The addition of other network modifiers (e.g., Li, K, Rb and Cs) can also increase diffusion. Each alkali addition creates additional NBOs that open up the network and reduce glass connectivity.

In more complex soda–lime glasses where the number of network modifiers is greater (e.g., CaO, MgO and K_2O), the effect of each modifier on the rate of exchange of OH^- with the alkali atom has not been fully quantified. However, Sinton and LaCourse (2001) indicate that the mechanism of exchange is still a two-stage process when in direct contact with aqueous media. In the first stage, there is an exchange at the surface between hydrogen and an alkali atom that follows the reaction

$$(\text{Si–O–R})_{\text{glass}} + H_2O \rightarrow (\text{Si–O–H})_{\text{glass}} + R^+ + OH^-_{\text{solution}}$$

In a closed system as time proceeds, the depletion of alkali and their transfer to solution, coupled with the increase in the concentration of OH^-, raises the pH and breaks the Si–O–Si bonds of the glass matrix and causes the glass to dissolve:

$$(\text{Si–O–Si})_{\text{glass}} + OH^- \rightarrow (\text{Si–OH})_{\text{glass}} + (\text{Si–O}^-)_{\text{solution}}$$

In an open system where the moisture is water vapour, dissolution may be delayed or avoided over long exposure periods.

Developing a predictive model of glass durability involves an identification of the network modifiers that either accelerate or retard the first-stage exchange process. Sinton and LaCourse (2001) have developed such a model to predict the rate of alkali exchange in a closed system for a fixed time at uniform temperature. Using the ISO static solution procedure (ISO 1985), crushed samples from 20 manufactured glasses were reacted with deionized water at 98°C for 1 h. The leachate was analysed by atomic absorption spectroscopy and stepwise regression analysis was used to quantify the relative effects of glass network modifiers on the exchange rate. The statistical analysis of the data set revealed that more durable glasses are those with low alkali content and a higher quantity of alumina. The addition of Na and K to the glass results in greater alkali exchange, with Na being preferentially leached out over the larger and slower-moving K^+ ion. The presence of alkaline earths such as CaO and MgO was not statistically significant in terms of enhancing or reducing durability.

The work of Sinton and LaCourse (2001) indicates that the leaching of soda–lime–silicate glasses behave in a predictable manner when exposed to solution and supports the goal of developing quantitative models to predict the leach rates for glasses of known composition. Archaeological samples, however, reside in open systems with a changing moisture environment and normally in vapour conditions where the relative humidity is less than saturated. Therefore, in this research we approach the problem of developing a predictive model of glass hydration from the perspective of quantifying how much water (H_2O) enters the glass structure rather than attempting to quantify the amount of alkali removed from the glass matrix.

Recent research by Cummings *et al*. (1998) has completed a series of vapour hydration experiments on a soda–lime–silicate glass containing network modifiers of CaO, K_2O, MgO and Na_2O. In all exposures at temperatures below 100°C, nuclear reaction analysis of the hydrated surface layer indicated that the depth of hydration proceeded with the square root of time. In addition, as the relative humidity was reduced, the rate of water diffusion decreased in a linear manner. In this analysis, we have conducted a series of low-temperature hydration experiments (< 190°C). We use secondary ion mass spectrometry (SIMS) and Fourier transform infrared spectroscopy (FTIR) to monitor the water diffusion and to determine if the water diffusion coefficients parallel the compositional effects on durability as determined from leaching experiments.

GLASS COMPOSITION

A large number of glass forms and compositions have been used over the past four centuries. In this study, we focus upon dark olive-green coloured wine bottle glasses because of their wide distribution and high frequency within the archaeological record (Fig. 1). The full glass compositional range for this container type remains poorly documented within the Americas and relatively few compositionally based studies of historic period glasses have been conducted. Robert Brill (1999) recently published a pair of volumes that compiled 39 years of research on the chemical analysis of glasses from around the world. Only one of these was a dark olive-coloured wine bottle of unprovenanced origin but thought to be from the Americas (Brill #502; *c*. 1750–1800). Other glass samples from early American contexts included a fragment of green window glass from the Jamestown Glasshouse (Brill #4221, *c*. 1608–9) and a window glass fragment from the Jamestown Statehouse (Brill #4, *c*. 1669). The notable feature of all three samples was the high calcium content (21–22%) and the mid-range silica content (60–65%).

Figure 1 *A partially reconstructed Colonial wine bottle*.

Table 1 *Glass compositions from Virginia historic period sites*

Sample	*Provenance*	SiO_2	Na_2O	*MgO*	Al_2O_3	K_2O	*CaO*	TiO_2	Fe_2O_3	*MnO*	*Sum*	*Type*
DHR-140	44JC37 #3	50.18	2.04	4.35	5.52	5.11	30.16	0.22	1.92	0.16	99.66	A-1
DHR-143	44PG151 #8	53.99	1.98	2.97	3.81	3.95	31.06	0.17	1.30	0.14	99.37	A-1
DHR-144	44PG151 #9	54.94	1.41	3.44	4.05	4.31	29.69	0.12	1.32	0.11	99.39	A-1
DHR-147	Kennon #15	55.76	2.21	4.60	4.66	4.59	25.94	0.19	1.54	0.17	99.66	A-1
DHR-139	Monticello #2	50.00	2.08	3.95	3.40	5.17	33.07	0.23	1.17	0.56	99.63	A-2
DHR-142	44CC178 #7	51.54	1.46	3.26	3.79	14.32	23.58	0.19	1.49	0.12	99.75	B
DHR-146	Jordans #13	51.48	1.03	2.9	2.52	13.67	26.84	0.15	0.94	0.23	99.76	B
DHR-138	Golden #1	57.32	2.22	3.93	3.95	0.63	29.97	0.17	1.46	0.07	99.72	C
DHR-145	44HE951 #11	60.35	3.79	4.00	4.52	1.01	24.19	0.39	1.46	0.15	99.86	C
DHR-141	44HE951 #6	58.36	3.03	0.86	8.02	4.19	24.16	0.16	1.07	0.03	99.88	D

In Europe, numerous investigations of 17th and 18th century glasshouses and glass waste have been conducted (Ashurst 1970; Crossley and Aberg 1972; Dungworth 2005), and they document the production of clear and coloured glass forms. A study on the chemistry of late 16th century and early 17th century British green container glass, similar to the materials in this study, documents the wide use of high-calcium glasses (CaO 17.9–28.5%) during this period (Cable and Smedley 1987). According to the authors, the colour and composition of this glass was accepted from the Medieval Period up to the late 19th century.

To examine the compositional range of glass constituents in green wine bottles, we selected a suite of ten shards from archaeological contexts ranging in date from 1630 to 1860 (Table 1). Analysis of the major and minor oxides was conducted by laser ablation—inductively coupled plasma—mass spectrometry (LA–ICP–MS) (Speakman and Neff 2005). The documented compositional range was significant within the major oxides that included a 10% range for both SiO_2 (50.00–60.35%) and CaO (23.58–33.07%). Al_2O_3 (3.40–8.02%) was generally in the 3–5% range, except for one high-aluminium sample. Na_2O (1.03–3.79%) was generally low. MgO (0.86–4.35%), Fe_2O_3 (0.94–1.92%), MnO (0.03–0.56%) and TiO_2 (0.12–0.39%) were present in reduced quantities. Although there is not a quantitative trend, the later period glasses tend to have more silica.

The consistently high proportions of calcium are the result of manufacturing preferences that used wood ash as a component in the glass recipe. Recent experiments have shown that an addition of oak, beech or bracken ashes increases the alkali content and lowers the melting temperature (Jackson and Smedley 2004). The exact amount of alkali would be difficult to determine precisely during glass manufacture, since the concentration of alkali within the ash varies between, and even within, tree species (Turner 1956). Consequently, the final chemistry of a glass will vary in oxide proportions and this will effect its interaction with water. For this reason, we have adopted a modelling approach that takes this chemical variation into account.

Although the sample of analysed glasses was small, a principal component analysis was conducted to illustrate the variation in the data. Figure 2 shows a biplot, with the first two components derived from the variance–covariance matrix for the eight major elements. The first component expresses enrichment of potassium and dilution of sodium, whereas the second component expresses enrichment in aluminium and dilution of magnesium and manganese.

Five compositional groups representing at least four glass-making recipes were identified (Table 1). Glass designated as Type A-1 is represented by four samples. Type A-2 differs from

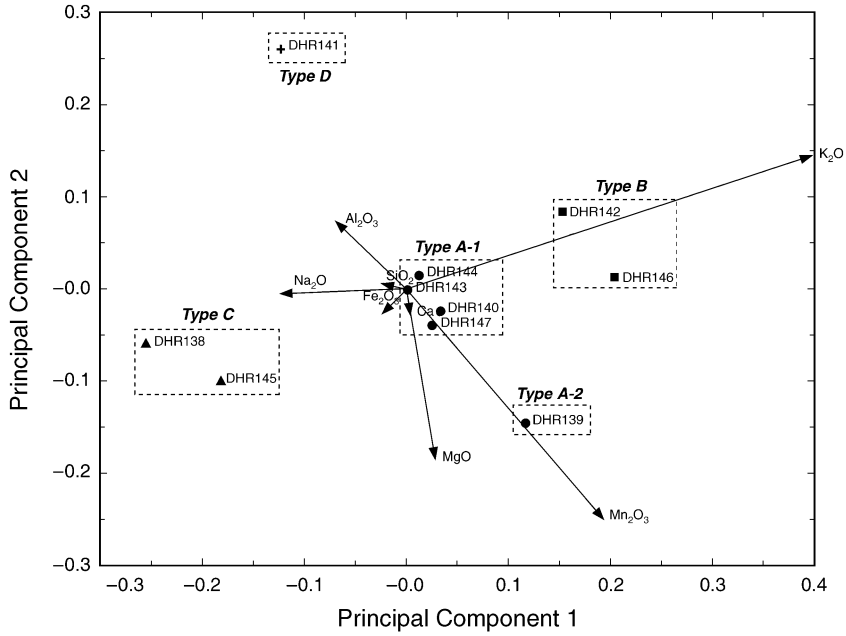

Figure 2 *Principal component analysis of high-calcium glasses.*

A-1 in that the sample is slightly higher in manganese and calcium and may reflect different types or sources for the stabilizer. Type B is represented by two samples and has lower sodium and significantly higher potassium than all the other groups. Type C is also represented by two samples and is distinguished by relatively lower potassium concentrations. Type D is represented by one sample and is characterized by lower magnesium and manganese and higher aluminium concentrations. From this set of five chemical groups, a single specimen from each (DHR-138, DHR-139, DHR-140, DHR-141 and DHR-147) was selected for experimental hydration.

EXPERIMENTAL HYDRATION OF HIGH-CALCIUM GLASSES

The development of a diffusion-based dating method requires that the reaction between water and the glass be quantified through empirical experiments. Previous investigations with a variety of natural and manufactured glasses (Friedman and Long 1976; Stevenson *et al*. 1998; Doremus 2002) have shown that the rate of water diffusion is exponentially dependent upon temperature and can be described by the Arrhenius equation (Arrhenius 1889):

$$\ln K = \ln A - E_a/RT$$

where K is a rate constant, A is the pre-exponential, E is the activation energy (KJ mol^{-1}), R is the universal gas constant (8.314 kJ mol^{-1} K^{-1}) and T is the temperature in degrees Kelvin.

The analysis below establishes the rate constants (K) and activation energies (E) through separate experiments. The rate constants were established by the hydration of glasses at a single temperature (80°C) at predefined exposure periods (60–240 days) and described by the slope of the regression line. The activation energy (E) and pre-exponential (A) were determined by plotting ln K versus $1/T$ to determine the slope ($-E/R$) and the y-intercept (ln A).

Sample preparation

Sample thick sections were prepared from large archaeological glass fragments that included the basal sections and thick sidewall portions of wine bottles. A slow-speed saw was used to cut parallel-sided, 1–2 mm wide slabs. Each slab was polished on both sides with a series of grits (180, 240, 400, 600 and 800) on a rotary polisher to produce a reflective surface. The samples were washed with demineralized water and allowed to air dry before repackaging.

Vapour hydration

Vapour hydration was conducted at temperatures ranging from 60°C to 190°C. In experiments with temperatures below 100°C, the hydration containers consisted of 125 ml polypropylene bottles. Each bottle contained one sample that was suspended by Teflon thread over 10 ml of demineralized water. There was no contact between the sample and the water phase at the base of the bottle. For experimental runs of 100–120°C, a durable one-litre polypropylene container was utilized. Five samples were suspended from sealed access ports on the lid over 50 ml of demineralized water. For samples reacted above 120°C, a one-litre Parr pressure reactor fitted with an additional thermal jacket was used. Samples were suspended over 200 ml of water from a stainless steel support using Teflon thread. A larger amount of water was used in the reaction vessel to stabilize the temperature readings registered by the thermocouples. The sample reactions at temperatures at or less than 120°C were conducted in convection ovens with a precision of ±0.5°C. The temperature variation within the Parr vessel is estimated to be ±1°C.

The 80°C samples were removed at approximately 30-day intervals after an initial 60 days of exposure had been completed. The maximum duration of hydration was 240 days. Higher-temperature runs at 100°C and 120°C were removed at 154 and 128 days, respectively. The experiments conducted at 150°C and higher were removed after a predetermined reaction period up to 30 days in duration (Table 2). After each hydration period, the samples were removed from the oven and allowed to cool to room temperature. This cooling process was accelerated by first opening the warm container and removing the samples. The specimens were then wiped with a soft tissue and allowed to air dry. Samples hydrated in the Parr reaction vessels were allowed to cool to room temperature over a period of 2 h after power to the vessel was shut off. The temperature of the reaction vessel drops in a near exponential manner, thus significantly reducing the contribution of additional hydration beyond the predetermined reaction period.

Analytical instrumentation and procedures

Water within bulk soda–lime–silicate glasses consists principally of hydroxyl (OH) when concentrations are less than 1000 ppm (Acocella *et al*. 1984; Geotti-Bianchini and De Riu 1995). In lower-calcium glasses (CaO ~ 10%) of this type, three infrared bands have been documented (Geotti-Bianchini *et al*. 1999) and include: (a) free hydroxyl band at 3570 cm^{-1}, formed by Si–OH pairs located with network voids of the silica structure; (b) a bonded hydroxyl band at 2777 cm^{-1} where Si–OH pairs bond with adjacent NBOs; and (c) another bonded hydroxyl band at 2325 cm^{-1}. In an unhydrated soda–lime–silicate available to us (Fig. 3, Curve A) the ~3523 cm^{-1} and ~2852 cm^{-1} peaks in the transmission spectra are readily observable. The ~2325 cm^{-1} is not visible and many times can only be identified by subtracting the spectra of a water free sample. The infrared transmission spectra of a high-calcium glass

Table 2 *Pre- and post-hydration absorbance values*

Sample no.	*Glass type*	*Temperature (°C)*	*Days*	*Pre-absorbance*	*Post-absorbance*	*Increase/2*
DHR-80	Monticello	80	59.41	0.2308	0.2518	0.0105
DHR-81	Monticello	80	89.29	0.1913	0.2197	0.0142
DHR-82	Monticello	80	120.25	0.2086	0.2440	0.0177
DHR-83	Monticello	80	150.25	0.1733	0.2710	***0.0489***
DHR-84	Monticello	80	180.25	0.2084	0.2553	0.0235
DHR-85	Monticello	80	210.25	0.2321	0.2806	**0.0243**
DHR-86	Monticello	80	240.07	0.1879	1.3099	***0.5610***
DHR-116	Kennon	80	59.41	0.1690	0.1913	0.0112
DHR-117	Kennon	80	89.29	0.1767	0.2016	0.0125
DHR-118	Kennon	80	120.25	0.2254	0.2683	***0.0215***
DHR-119	Kennon	80	150.25	0.2070	0.7233	***0.2582***
DHR-120	Kennon	80	180.25	0.1690	0.2032	0.0171
DHR-121	Kennon	80	210.25	0.1995	0.5574	***0.1790***
DHR-122	Kennon	80	240.07	0.1634	2.0400	***0.9383***
DHR-73	Golden Ball	80	59.41	0.2570	0.2743	0.0086
DHR-74	Golden Ball	80	89.29	0.1928	0.2146	0.0109
DHR-75	Golden Ball	80	120.25	0.2039	0.2291	0.0126
DHR-76	Golden Ball	80	150.25	0.2025	0.2307	0.0141
DHR-77	Golden Ball	80	180.25	0.1697	0.2030	0.0167
DHR-78	Golden Ball	80	210.25	0.1667	0.3711	***0.1022***
DHR-79	Golden Ball	80	240.07	0.1836	1.5403	***0.6784***
DHR-87	44JC37	80	59.41	0.1853	0.2006	0.0077
DHR-88	44JC37	80	89.29	0.2116	0.2305	0.0095
DHR-89	44JC37	80	120.25	0.2614	0.2875	0.0131
DHR-90	44JC37	80	150.25	0.2621	0.2878	0.0129
DHR-91	44JC37	80	180.25	0.2092	0.2368	0.0138
DHR-92	44JC37	80	210.25	0.2098	0.8157	***0.3030***
DHR-93	44JC37	80	240.07	0.2570	1.8350	***0.7890***
DHR-123	44HE951	80	59.41	0.1876	0.1994	0.0059
DHR-124	44HE951	80	89.29	0.1798	0.1932	0.0067
DHR-125	44HE951	80	120.25	0.1731	0.1894	0.0082
DHR-126	44HE951	80	150.25	0.1665	0.1830	0.0082
DHR-127	44HE951	80	180.25	0.2158	0.2368	0.0105
DHR-128	44HE951	80	210.25	0.1917	0.2136	0.0110
DHR-129	44HE951	80	240.07	0.2400	0.2652	0.0126

(DHR-328, Curve B) shows that only a 3561 cm^{-1} band is resolved in the unhydrated bulk glass and the glass slab with hydrated surface layers (Curve C). The presence of only the peak at 3561 cm^{-1} in all of the experimental samples implies that OH has not bonded with the glass structure. In addition, a molecular water band at 1620 cm^{-1} (Geotti-Bianchini and De Rui 1995) was not observed during any of the analyses.

Measurement of the surface absorbed water was conducted with a Bomem-120 Fourier transform infrared spectrometer (FTIR). Standard absorbance measurements were made using a total of 100 scans collected at 8 cm^{-1} resolution with a 7 mm aperture. The OH peak at 3561 cm^{-1} was monitored to quantify both the initial structural water present in the glass before reaction and the amount of hydroxyl that had diffused into the sample surface during hydration.

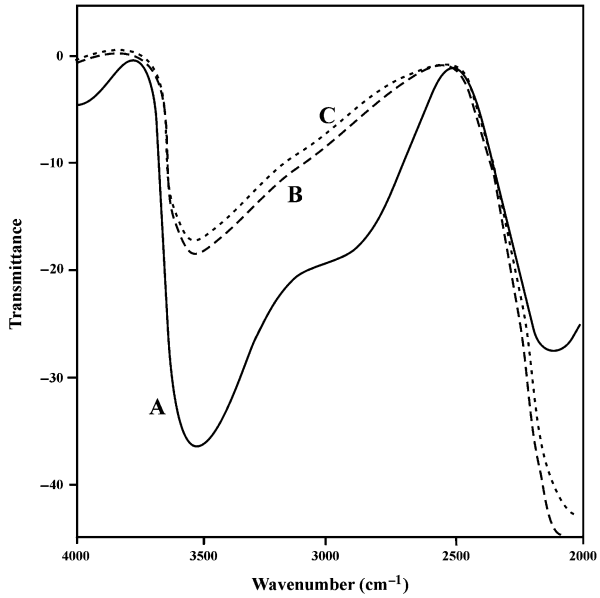

Figure 3 *Infrared transmission spectra of an unhydrated soda–lime glass (A), a hydrated high-calcium glass (B) and an unhydrated high-calcium glass (C).*

Absorbance values were not converted to weight per cent water concentrations because they were suitable analytical units.

A selected number of hydrated surfaces from either archaeological context (DHR-301, DHR-309) or from laboratory hydration (DHR-91, DHR-93) were depth profiled using secondary ion mass spectrometry (SIMS). The SIMS analysis was performed in order to find the point of inward water diffusion located at the full-width at half-maximum (FWHM) point on the hydrogen profile and to monitor the extent of leaching associated with the more mobile alkali ions (e.g., CaO, K_2O and Na_2O). The analyses were performed using a PHI Model 6600 quadrupole-based secondary ion mass spectrometer at Evans East. A 5.0 KeV Cs^+ primary ion beam with an impact angle of 60° with respect to surface normal was used and negative secondary ions were detected. Charge build-up during profiling was compensated for by use of an electron beam. The ion signal was maximized by an electron beam to find the least amount of charging. The measurements were performed using a 300 × 300 μm ion beam raster, which results in very little visual disruption to the sample surface. Generally, the SIMS depth scale accuracy is within 5–10%. This translates into an estimated error of ±0.05 μm.

ANALYTICAL RESULTS

Arrhenius constants

The rate constants for the five glass samples were calculated by plotting the absorbance values for each of the glass specimens (Table 2) as a function of time within the reaction vessels (Fig. 4). Zero intercept values were added to the data set prior to analysis. The linearity of these plots indicates that the reaction kinetics follow the 1-D diffusion model. The diffusion of

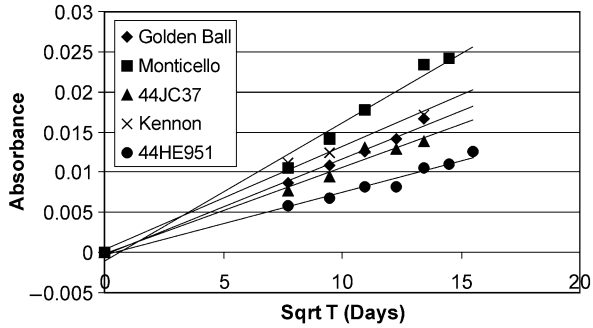

Figure 4 *Absorbance values versus the square root of time (days).*

Table 3 *Pre-exponential and activation energy values for high-calcium glasses*

Lab. no.	*Glass type*	*A [(absorbance units)^2 per day]*	*E (kJ mol^{-1})*
DHR-139	Monticello (#2)	2.89×10^{-6}	28.747
DHR-147	Kennon (#15)	1.69×10^{-6}	35.016
DHR-138	Golden Ball (#1)	1.44×10^{-6}	36.608
DHR-140	44JC37 (#3)	1.21×10^{-6}	40.482
DHR-145	44HE951 (#6)	0.64×10^{-6}	43.733

water in all of the glass compositions progressed with the square root of time and formed linear calibrations with correlation coefficients greater than $r^2 = 0.96$. The magnitude of the rate constants ranged from 0.64×10^{-6} to 2.89×10^{-6} (absorbance units)^2 per day or (mass change)^2 per day (Table 3).

Several problems were encountered in the analysis of these long-term exposures at 80°C. Most of the samples hydrated for durations less than 210 days behaved in a predictable and regular manner, with incremental changes in absorbance with time. However, three of the samples (DHR-83, DHR-118 and DHR-119) had significantly greater quantities of diffused surface water than expected from the overall trend, which cannot be explained solely by experimental error (Table 2). In these cases, the observed absorbance values were greater than the adjacent values by a factor of at least two. We attribute this to condensation on the surface of the specimen that accelerated the hydration process.

A similar phenomenon was observed in four glass sample sets that were exposed to water vapour up to 240 days (Table 2). Here, the increases in absorbance values for the longest of the samples (210 and 240 days) were many orders of magnitude greater than the trend defined by samples reacted for shorter durations. An examination of why this might have occurred led to a microscopic examination of the sample. The surface of each sample exhibiting this rapid increase in diffused water had become ruptured and irregular in surface texture (Figs 5 and 6). This increased the effective surface area and increased the rate of water absorbance. It was hypothesized that the structure of the glass had begun to break down as a result of the removal of mobile ions from the near-surface region. SIMS element profiles were used to characterize the evolution of this surface (see below).

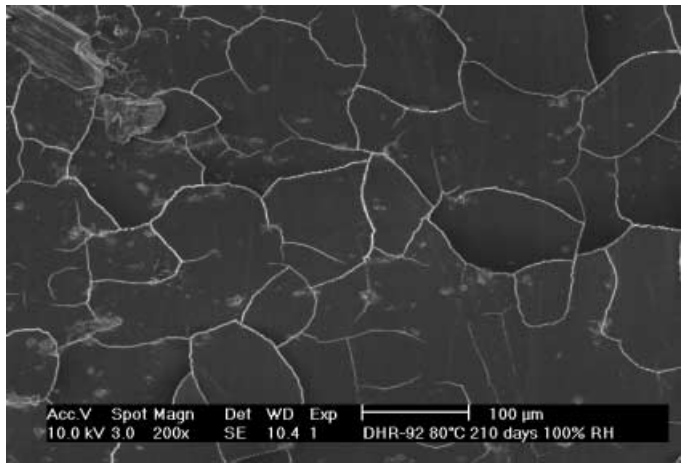

Figure 5 *A deteriorated hydrated surface of high-calcium glass, showing extensive surface cracking after 210 days of hydration.*

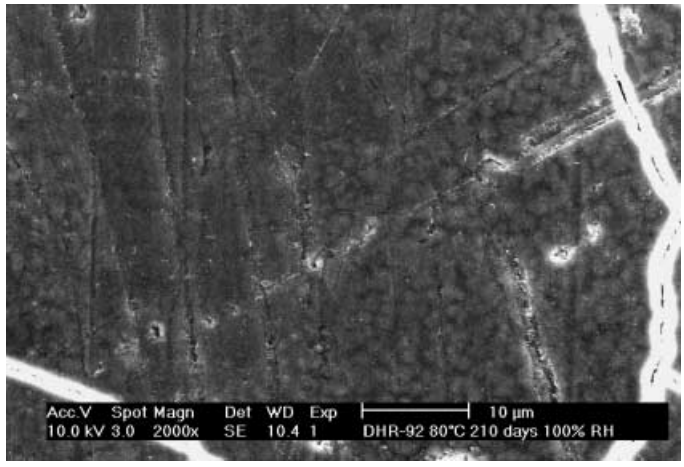

Figure 6 *A hydrated surface of high-calcium glass, showing surface cracking after 210 days of hydration.*

Activation energy values for the five sample sets were determined through a correlation of the natural log of the absorbance values [LN (Abs)] with an inverse of the reaction temperature in degrees Kelvin (Table 4). The slopes of the regression lines resulted in activation energy determinations between 28.7 and 43.7 kJ mol^{-1} (Fig. 7).

Hydrogen diffusion profiles

SIMS hydrogen profiles were collected on two specimens. The first was a normal sample hydrated at 80°C for 180.25 days that incorporated water according to $t^{1/2}$. The second was on a sample that had become superhydrated after an exposure of 240.07 days at 80°C. The SIMS element profiles in Figure 8 show that glass type 44JC37 (180.25 days) has an error function

Table 4 *Activation energy absorbance data*

Sample no.	*Glass*	*Temperature (°C)*	*Days*	*Pre-absorbance*	*Post-absorbance*	*Increase*	*LN (absorbance units per day)*
DHR-81	Monticello	80	89.29	0.1952	0.2002	0.0050	−9.7902
DHR-101	Monticello	100	154.15	0.1934	0.2071	0.0137	−9.3282
DHR-98	Monticello	120	128.25	0.2068	0.2239	0.0171	−8.9226
DHR-95	Monticello	150	29.95	0.1700	0.1758	0.0058	−8.5494
DHR-327	Monticello	170	20.00	0.2215	0.2300	0.0085	−7.7634
DHR-68	Monticello	180	15.00	0.1214	0.1291	0.0077	−7.5745
DHR-134	Kennon	100	154.15	0.1918	0.2114	0.0196	−8.9702
DHR-132	Kennon	120	128.25	0.1733	0.1990	0.0257	−8.5152
DHR-130	Kennon	150	29.95	0.1586	0.1732	0.0146	−7.6263
DHR-215	Kennon	160	18.01	0.1796	0.1981	0.0185	−6.8809
DHR-325	Kennon	170	20.00	0.2194	0.2340	0.0146	−7.2225
DHR-217	Kennon	190	18.01	0.2005	0.2200	0.0195	−6.8283
DHR-100	Golden Ball	100	154.15	0.1467	0.1629	0.0162	−9.1606
DHR-97	Golden Ball	120	128.25	0.1666	0.1916	0.0250	−8.5428
DHR-94	Golden Ball	150	29.95	0.1906	0.2040	0.0134	−7.7120
DHR-328	Golden Ball	170	20.00	0.2167	0.2300	0.0133	−7.3157
DHR-90	44JC37	80	89.29	0.2250	0.2305	0.0055	−9.6949
DHR-102	44JC37	100	154.15	0.2212	0.2407	0.0195	−8.9753
DHR-99	44JC37	120	128.25	0.2002	0.2340	0.0338	−8.2413
DHR-42	44JC37	150	15.00	0.1390	0.1478	0.0088	−7.4411
DHR-26	44JC37	160	15.19	0.2831	0.2958	0.0127	−7.0868
DHR-326	44JC37	170	20.00	0.2055	0.2250	0.0195	−6.9331
DHR-137	44HE951	60	251.31	0.2034	0.2111	0.0077	−10.393
DHR-128	44HE951	80	210.00	0.1917	0.2136	0.0219	−9.1684
DHR-135	44HE951	100	154.15	0.1850	0.2197	0.0347	−8.3989
DHR-133	44HE951	120	128.25	0.1799	0.2216	0.0417	−8.0312
DHR-131	44HE951	150	29.95	0.1886	0.2198	0.0312	−6.8669
DHR-324	44HE951	170	20.00	0.1966	0.2325	0.0359	−6.3228

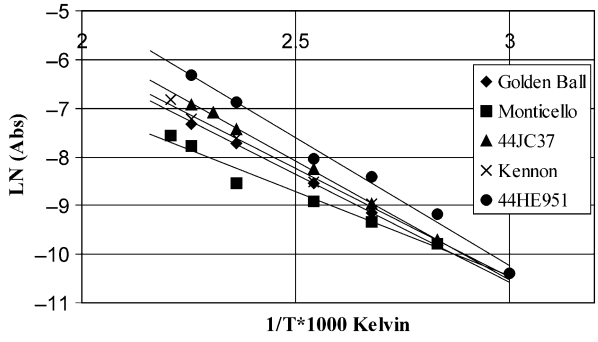

Figure 7 *Activation energy plots for high-calcium glasses.*

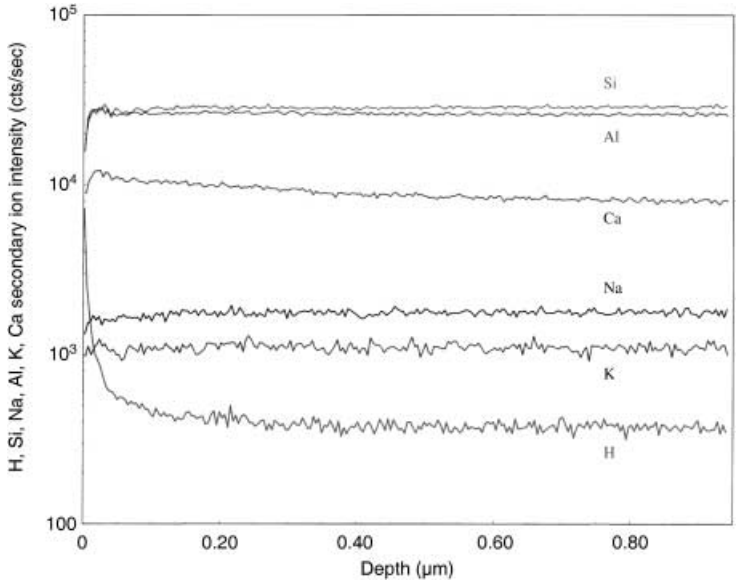

Figure 8 *Element profiles for glass 44JC37 hydrated at 80°C for 180.25 days.*

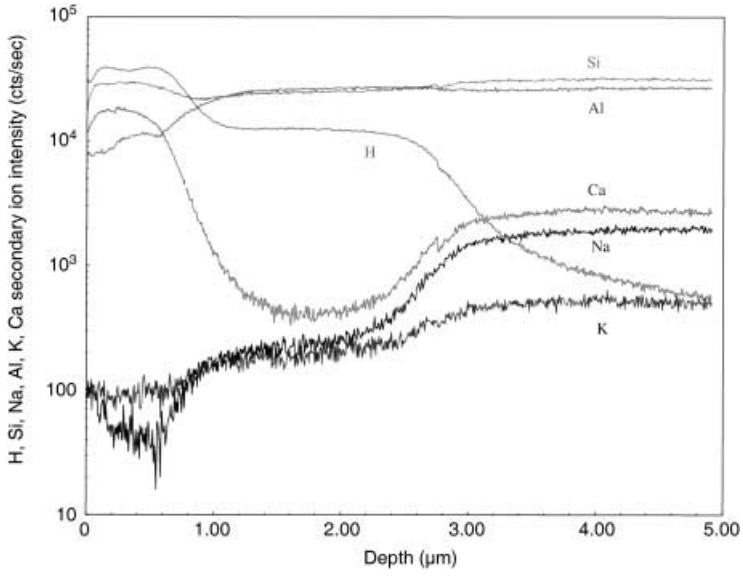

Figure 9 *Element profiles for glass 44JC37 hydrated at 80°C for 240.07 days.*

type hydrogen profile that reaches a depth of 0.20 μm. Calcium shows a slight enrichment near the surface and sodium is very slightly depleted at a depth of 0.10 μm. The remaining element profiles are unchanged between the bulk and the near-surface region.

The hydrated region on the 44JC37 glass hydrated for 240.07 days at the same temperature shows a radically different element profile (Fig. 9). The hydrogen profile exhibits two

plateaus. The first plateau is from the surface to a depth of 0.8 μm at the FWHM point and the second plateau extends to a depth of approximately 3.0 μm. This represents the furthest inward point of water diffusion. Counterbalancing the hydrogen diffusion profile is a significant depletion of sodium and potassium at a depth of 2–3 μm that correlates with the front of the second hydrogen profile. Calcium has also been removed from the glass to a depth of 3 μm, but is highly concentrated in the region between 0 and 1 μm. In addition, sodium and potassium exhibit their maximum depletion in this region that correlates with the first hydrogen profile.

On the basis of published short-term leaching experiments of soda–lime glasses, neither of these profiles were anticipated, but they can be explained on the basis of glass chemistry and the changing structure of the glass. In the earlier stages of water diffusion (180.25 days) for the 44JC37 glass, the low amount of sodium (2.04%) permits only a very small amount of water to enter the glass structure and, as such, a stepped hydrogen concentration profile has not developed. The diffusion at this stage is very minimal. However, an extrapolation of this trend in water diffusion to 240.07 days does not explain the magnitude of the hydration that is demonstrated by the SIMS profile. Between 180 and 240 days there is a clear and rapid change in the leaching process that involves much more than the simple one-to-one exchange between sodium and water.

The presence of a double hydrogen plateau and depletion, or enrichment in other elements, provides an explanation for this change in mechanism. We propose that the surface of the glass becomes rapidly superhydrated as a result of extended leaching of sodium, calcium and potassium, in the near-surface region (< 1 μm). A significant loss of silica is also documented. This extended leaching actually reflects a severe degradation of the glass structure that significantly increases the glass porosity and allows a larger amount of water to accumulate at the surface. This high concentration greatly increases the water diffusion rate and results in the rapid formation of the 3 μm deep hydration layer. The presence of this phenomenon in the four least durable glasses suggests that a threshold is reached that triggers the rapid ion exchange process. The slowest hydrating 44HE951 glass was not subject to the rapid ion exchange.

SIMS element profiles were also acquired from two archaeological glass samples (DHR-301 and DHR-309) from the late 18th to early 19th century site of Monticello. The glasses are of the same composition and within analytical error associated with LA–ICP–MS. The samples were recovered from sediments within a domestic dwelling (see below).

Sample DHR-301 exhibits the same profile configuration as collected from the early stage 80°C experimental samples (Fig. 10). The hydrogen profile has an error function shape and sodium exhibits some very minimal depletion. This sharply contrasts with artefact DHR-309 (Fig. 11). The surface of this sample is hydrogen-enriched at a higher concentration than the plateau of the hydrogen step-profile. Calcium, potassium and sodium are depleted at a depth of 0.3 μm, but also exhibit a pronounced enrichment at the surface. This is in contrast to the experimentally hydrated sample, in which sodium and potassium were severely depleted at the surface and calcium was enriched. In this case, the enrichment of all three oxides is interpreted to represent a surface precipitate, which—like the severely depleted region of the 240.07 day laboratory sample—is loosely consolidated and is able to maintain an elevated water concentration. This in turn increases the diffusion coefficient and causes the development of a stepped hydrogen concentration profile (Fig. 9). The comparison of laboratory-hydrated samples and archaeological samples reveals that accelerated diffusion coefficients can arise from very different processes that generate a high surface-water concentration.

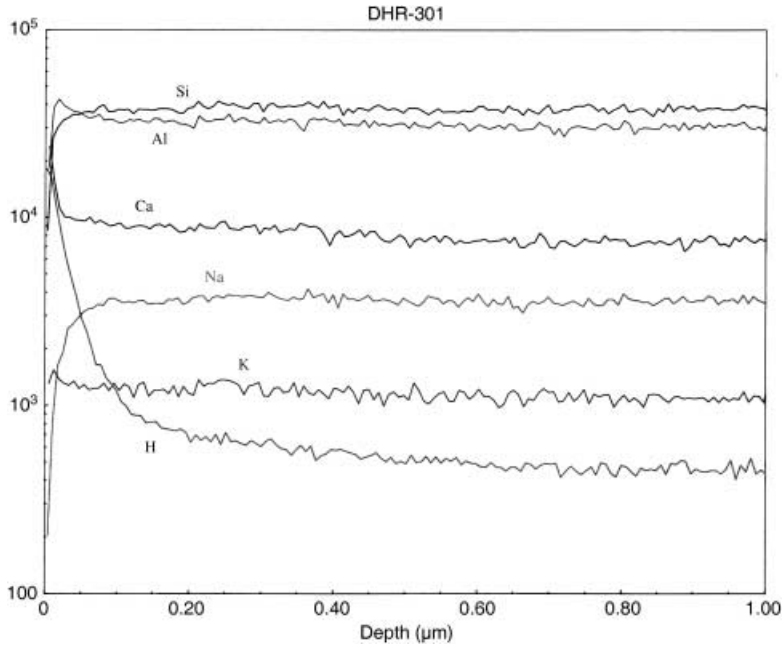

Figure 10 *SIMS element profiles on an archaeological wine bottle fracture surface (DHR-301).*

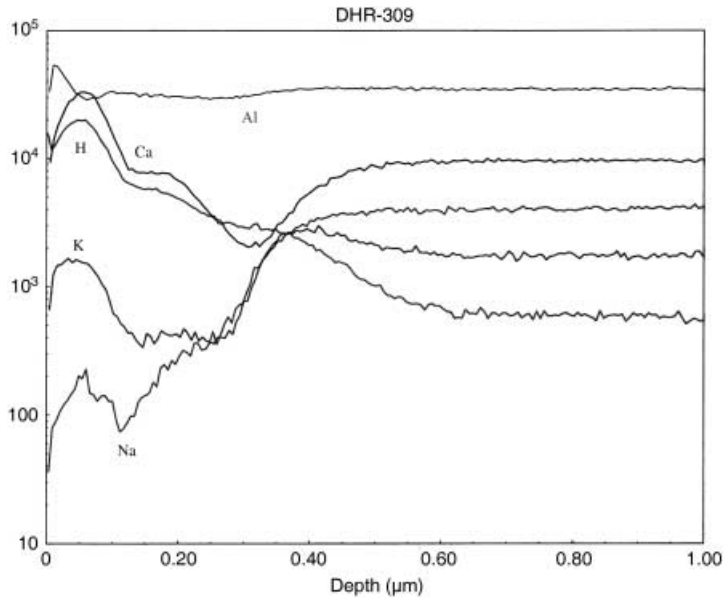

Figure 11 *SIMS element profiles on an archaeological wine bottle fracture surface (DHR-309).*

The chemical dependence of hydration

A large body of data exists on the durability of glasses, but few of these studies have examined high-calcium glasses similar to the ones investigated here. However, the studies that have

been conducted are informative. The leaching experiments of El-Shamy *et al*. (1975) in Na_2O–CaO–SiO_2 glasses in acidic solutions revealed that in low-calcium glasses sodium was preferentially leached out over calcium. However, as calcium increased above 10 wt%, uniform leaching of the oxide components was observed. Melcher and Schreiner's (2005) investigation of a high-calcium glass (60% SiO_2 – 25% CaO – 15% K_2O) that was naturally weathered by exposure to the atmosphere over long time periods (1–6 years) revealed that potassium is preferentially leached out over calcium by as much as 10%. This is attributed to the higher bond strength of the bivalent calcium ion to the non-bridging oxygen sites in the glass. It therefore appears that, under several different conditions, sodium and potassium are more mobile than calcium and are depleted preferentially to calcium.

The SIMS hydrogen profiles on our high-calcium glasses hydrated for short durations show only a very slight leaching of sodium. At longer durations the SIMS profiles qualitatively show the congruent leaching of all three mobile network modifiers. The decline in the oxide concentrations for CaO, K_2O and Na_2O all have nearly identical inflection points on their respective element profiles near the 3.0 μm depth on the experimental samples (Fig. 9). However, on archaeological sample DHR-309, sodium and potassium show more extensive depletion (Fig. 11). We have used these observations as a guide to modelling the chemical dependence of water diffusion into the surface of the experimental glasses.

Prior to developing the predictive model, the quality of the chemical data was re-evaluated. The LA–ICP–MS analysis of the samples in the first phase of the project was sufficient to identify general glass types even though the precision was estimated to be 5–7%. To increase the precision for short half-life elements, the five experimental glass samples were re-analysed by instrumental neutron activation analysis (INAA) according to Glascock (1998) (Table 5). For Al_2O_3, CaO, K_2O and MnO the precision was improved to 2–3%, and for Na_2O the precision was improved to 3–4%.

This reduction in analytical error would aide in the identification of meaningful trends within the data. SiO_2, MgO and Fe_2O_3 were not quantified by INAA because of the poor sensitivity for these elements by the procedure employed Therefore, the previous values for these constituents determined by LA–ICP–MS were retained.

The potential of individual oxides to predict the pre-exponential was examined (Fig. 12). Six correlations were performed with Al_2O_3, CaO, K_2O, MnO, Na_2O and SiO_2. Except for Al_2O_3, the correlations were weak and r^2 values ranged between 0.15 and 0.89. The correlation for Al_2O_3 revealed a strong inverse relationship ($r^2 = 0.97$) where the magnitude of the pre-exponential decreased with increasing Al_2O_3. The relationship is non-linear and the best-fit line is a power function ($x^{-0.7783}$). This confirmed previous studies that identified alumina as very influential in increasing glass durability and retarding ion exchange (Wassick *et al*. 1983).

Table 5 *Predictor oxide values for experimentally hydrated glasses*

Glass type	*Na_2O*	*Al_2O_3*	*K_2O*	*CaO*
Monticello (#2)	2.00	2.47	2.95	28.34
Kennon (#15)	2.18	3.57	2.54	21.74
Golden Ball (#1)	2.18	3.69	0.45	26.81
44JC37 (#3)	1.85	5.24	2.43	23.71
44HE951 (#6)	3.14	7.74	2.13	21.91

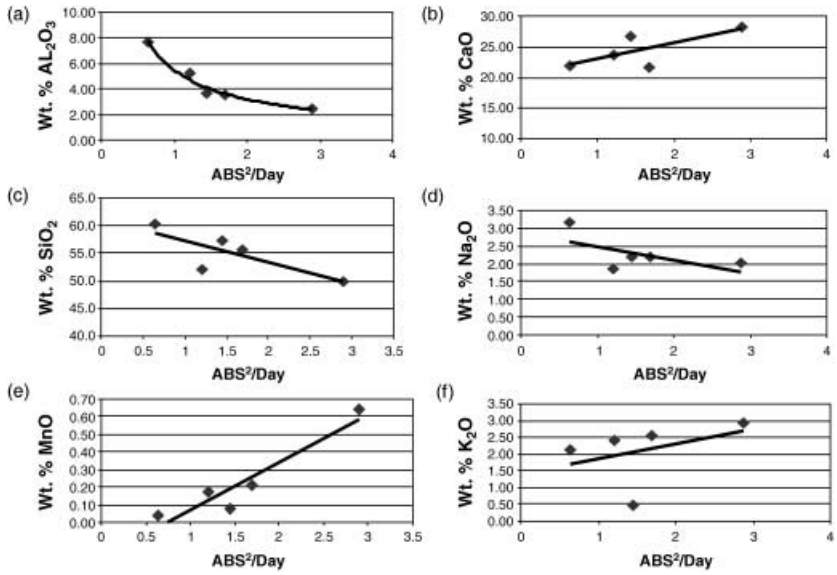

Figure 12 *Correlations between the glass rate constants and the compositional constants: (a) $R^2 = 0.965$; (b) $R^2 = 0.5247$; (c) $R^2 = 0.6221$; (d) $R^2 = 0.3581$; (e) $R^2 = 0.8898$; (f) $R^2 = 0.1472$.*

Table 6 *Regression weighting values for the pre-exponential and activation energy*

Oxide	*Pre-exponential*	*Activation energy*
Al_2O_3	−0.0004	3960.88
CaO	0.0003	−205.47
K_2O	0.0003	911.82
Na_2O	0.0001	−1386.24

A stepwise linear regression was performed with the SYSTAT statistical package to develop prediction equations for the activation energy and pre-exponential coefficients. The predictor variables included Al_2O_3, CaO, K_2O and Na_2O. Al_2O_3 was included because of the strong inverse relationship with the magnitude of the pre-exponential, and CaO, K_2O and Na_2O were included because they were identified in the SIMS analysis as the three most mobile oxides. The inclusion of these variables explained 100% of the variance within the experimental data set. The weighting factors for each variable are listed in Table 6.

APPLICATION OF THE DATING METHOD

The development of diffusion-based dating procedures in the laboratory requires validation with archaeological case examples. In contrast to laboratory conditions, archaeological contexts are a source of numerous intervening variables that can alter the diffusion process or the surface integrity of the archaeological glass. For example, aggressive alkaline environments can lead to surface dissolution and recycling and re-deposition can complicate the thermal history of the artefact. Many of these potential problems can be minimized by sample selection

after careful evaluation of archaeological context. A convergence in age estimates between the glass hydration dates and dates from other forms of material culture and historical documents will demonstrate the potential of the laboratory calibrations.

Sample context

As a first test of the methodology, artefacts from Building o at the historic period site of Monticello (1750–1850) will be dated. President Thomas Jefferson initiated the construction of the Monticello plantation in 1769, and for the next 50 years of his life he significantly altered the landscape by the creation of formal gardens, terraced vegetable gardens and extensive agricultural fields. The results of Jefferson's innovative agricultural experiments and construction activities are now the focus of intensive study by Monticello archaeologists. Their work has resulted in the development of a four-phase chronology for the plantation, based in part upon the calculation of Mean Ceramic Dates and nail manufacturing technology:

- Phase I, 1750–70: Monticello used by Peter Jefferson as an outlying farm.
- Phase II, 1770–90: Thomas Jefferson establishes his home farm.
- Phase III, 1790–1805: agricultural diversification and relocation of slave quarters.
- Phase IV, 1805–26: further dispersal of quarter sites.

A method used widely by historical archaeologists for dating archaeological contexts is the Mean Ceramic Date (MCD). First introduced by Stanley South in 1972, MCDs calculate the median date of occupation for a site or deposition for individual contexts. The MCD is calculated by first multiplying the number of shards of each ceramic type by its median date of manufacture. Next, the products are summed. The last step is to divide the sum of the products by the total number of shards. The resulting number represents the year for the median date of occupation. The median manufacturing date is determined primarily from documentary sources:

$$\bar{x} = \left(\sum_{i=1}^{n} f_i m_i \right) \Big/ \left(\sum_{i=1}^{n} f_i \right)$$

where f is the frequency of occurrence and m is the median date of manufacture for the ceramic type in question.

Despite the proximity of Building o to Jefferson's mansion and its original kitchen, the construction and demolition of the log cabins on the site received little comment in his personal documents. A single glimpse is afforded by Jefferson's 1796 Mutual Assurance Declaration: *o. a servant's house 20^{1}/$_{2}$ f. by 12 f. of wood, with a wooden chimney, & earth floor*.

The architectural features uncovered during excavation (Kelso 1997) revealed three surviving fragments of stone foundation walls representing two distinct episodes of construction. Based on Mean Ceramic Dates, the first log cabin went up in the 1770s. This structure was destroyed by the early 1790s and was replaced by Building o, which Jefferson described in 1796. Construction and use of the second cabin obliterated almost all features of the first dwelling. Building o had a large, rock-lined, 5 ft by 8 ft sub-floor pit (Feature 6) and a contemporaneous brick-lined pit (Feature 5) on the eastern gable end (Fig. 13). However, the use of the second cabin was fairly short. The structure was dismantled and the base encapsulated by a layer of redeposited subsoil. The source of the deposit is probably from the 1801 excavation of the hillside between the mansion and the South Pavilion for the construction of the south dependency wing (DAACS 2004).

Archaeological investigations at Monticello have been extensive and have focused on the kitchen area of the main house and the slave quarters along Mulberry Row (Kelso 1986).

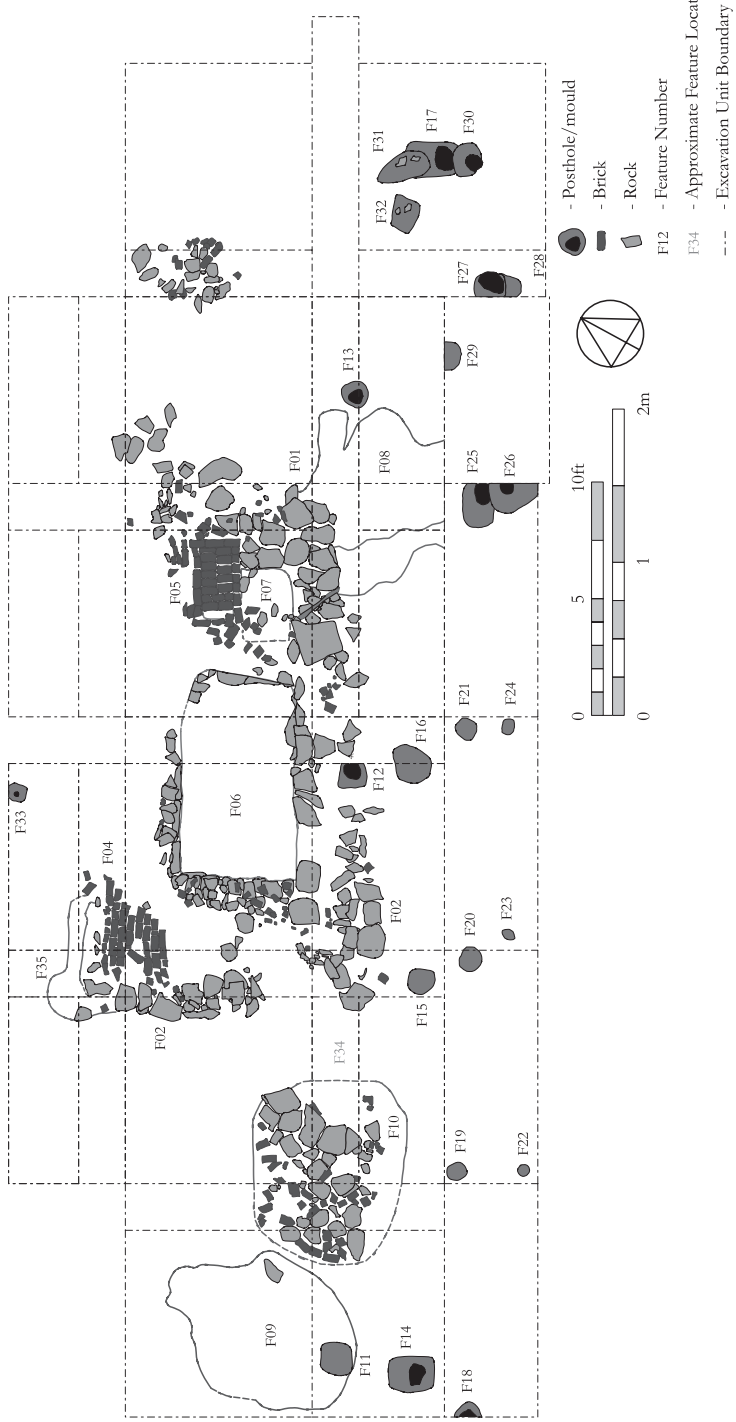

Figure 13 *A top plan view of Building o in Mulberry Row, Monticello.*

Samples to be dated in this analysis are wine bottle fragments recovered from floor and pit contexts within the slave dwelling labelled Building o (Fig. 13). The deposits within the structure are dated to 1760–1800, based upon a Mean Ceramic Date on over 1000 shards. The samples of wine bottle glass to be analysed came from deposits sealed by the redeposited subsoil. Most were located within the large, rock-lined sub-floor pit (see Fig. 13, feature 6 (F06)). The remainder were recovered from sediments within the structure that were indistinguishable from the sub-floor pit's fill.

Soil temperature and humidity

Water diffusion in glass is thermally activated and requires an estimated annual temperature for the artefact context. Soil relative humidity is equally important and if it is less than 100% the rate of water diffusion is slowed (Mazer *et al*. 1991; Friedman *et al*. 1994). Estimates for these variables were empirically determined at Monticello in 2002–3. Salt-based thermal and humidity monitors (Trembour *et al*. 1988) were buried at Mulberry Row for a complete annual cycle (379 days) at depths of 30, 60 and 90 cm below ground surface. The weight gain of the cells accumulated over the course of the exposure period was used to calculate an annual effective hydration temperature and relative humidity for each depth (Table 7). Because the wine bottle fragments from Building o were recovered from a depth of 60–80 cm, an annual effective temperature of 14.9°C and a relative humidity of 100% were used to calculate the archaeological diffusion coefficients for each archaeological glass artefact. These estimates are preferential to using meteorological surface data, but are still only a general guide that may not reflect the long-term annual mean for the past two centuries.

Glass composition, hydration layer measurement and age estimation

Thirteen wine bottle fragments were selected from sealed deposits within Building o. Thick sections were cut with a diamond blade trim saw from the larger sample and analysed for major and minor oxides by LA–ICP–MS and neutron activation analysis at the University of Missouri, Columbia, research reactor. Each of the wine bottle fragments was a high-calcium glass (21.5–34.03%) with low amounts of sodium (1.01–3.04%) and potassium (0.68–2.50%) (Table 8). A single sample (DHR-308) was of a composition that fell outside of the compositional range for the calibration samples. This artefact was different from the other samples because it contained high aluminium (8.34%) and lower calcium (21.50%) concentrations. This sample was eliminated from further analysis.

The amount of surface-diffused water was determined by infrared photoacoustic spectroscopy (PAS). An MTEC-300 photoacoustic cell was used in conjunction with the MB-120 infrared spectrometer. A 5–8 mm long section of each artefact fracture surface was cut with a diamond

Table 7 *Effective hydration temperatures and relative humidity values at Monticello*

Cell no.	*Depth (cm)*	*Days*	*Temperature (°C)*	*%RH*
7 & 8	30	379	15.5	100
17 & 18	60	379	15.1	100
19 & 20	90	379	14.8	100

Table 8 *Chemical compositions for Monticello Building o artefacts: entries in italics are analysed by LA–ICP–MS, and the remainder by neutron activation*

Lab. no.	*SiO_2*	*Na_2O*	*MgO*	*AL_2O_3*	*K_2O*	*CaO*	*Fe_2O_3*	*MnO*	*Sum*
DHR-301	*60.16*	2.02	*3.87*	4.67	0.86	27.56	*1.39*	0.07	100.6
DHR-302	*58.81*	1.01	*3.48*	4.66	2.18	27.57	*1.62*	0.15	99.5
DHR-303	*53.95*	1.64	*3.93*	5.03	0.77	32.41	*1.58*	0.05	99.4
DHR-304	*54.26*	1.62	*4.42*	5.67	2.50	27.99	*2.74*	0.14	99.3
DHR-305	*59.88*	1.08	*4.33*	4.30	2.01	25.94	*1.62*	0.14	99.3
DHR-306	*51.72*	1.67	*4.39*	5.25	0.57	34.03	*1.67*	0.06	99.4
DHR-307	*59.22*	1.35	*2.01*	4.15	1.79	29.88	*1.38*	0.11	99.9
DHR-308	*59.19*	3.04	*3.63*	8.34	1.14	21.50	*1.83*	0.61	99.3
DHR-309	*60.80*	1.97	*3.81*	4.74	1.55	26.46	*1.35*	0.05	100.7
DHR-310	*55.38*	1.65	*4.27*	5.30	0.68	30.67	*1.73*	0.05	99.7
DHR-311	*59.68*	2.41	*4.03*	5.37	0.80	26.86	*1.01*	0.12	100.3
DHR-312	*53.44*	1.59	*4.83*	5.54	2.14	29.47	*2.39*	0.15	99.5
DHR-313	*58.70*	1.04	*2.74*	5.03	1.80	29.38	*1.56*	0.15	100.4

Table 9 *Glass hydration dates for Monticello Building o artefacts: the standard deviation (S.D.) represents a 2σ estimated error*

Lab. no.	*Absorbance*	*EHT (°C)*	*%RH*	*A [(absorbance units)^2 per day]*	*E (J mol^{-1})*	*Rate [(absorbance units)^2 per year]*	*Date (AD)*	*S.D.*
DHR-301	0.0780	14.9	100	0.000001752	40653	0.0000280	1788	41
DHR-302	0.0763	14.9	100	0.000001850	41749	0.0000272	1791	40
DHR-303	0.0645	14.9	100	0.000001952	47044	0.0000191	1787	41
DHR-304	0.0000	14.9	100	0.000001767	45221	0.0000199	–	–
DHR-305	0.0839	14.9	100	0.000001801	38773	0.0000333	1793	40
DHR-306	0.0000	14.9	100	0.000001975	49394	0.0000161	–	–
DHR-307	0.0869	14.9	100	0.000002270	41440	0.0000342	1784	42
DHR-309	0.0849	14.9	100	0.000001808	39833	0.0000308	1771	44
DHR-310	0.0608	14.9	100	0.000001647	46523	0.0000168	1784	42
DHR-311	0.0682	14.9	100	0.000001502	42245	0.0000212	1786	41
DHR-312	0.0646	14.9	100	0.000001851	46162	0.0000194	1789	41
DHR-313	0.0693	14.9	100	0.000001779	44896	0.0000205	1771	44

blade trim saw to fit into the cell sample holder. The cell was purged with ultrapure helium filtered through a gas purifier cartridge to remove moisture. A desiccant (anhydrous magnesium perchlorate) was also placed below the sample cup floor to remove any adhering moisture. Two separate runs were made on each sample and consisted of the archaeological surface and a polished unhydrated surface on the rear of the same fragment. Each run consisted of 250 scans at a resolution of 16 cm^{-1}. Carbon black supplied by the manufacturer was used as the background reference material.

To determine an archaeological age, the absorbance values associated with the water peak at 3561 cm^{-1} of the unhydrated sample were subtracted from the absorbance associated with the hydrated surface. The net gain in absorbance was converted to an age using the calibrations developed above (Table 9). The error associated with absorbance measurements ranges from

Table 10 *Ceramic manufacturing midpoints and error ranges, and mean ceramic date for Building o sub-floorpit fill (feature 06)*

Ware	*Decorative technique type*	*Date range*	*Midpoint*	*Error range*	*Shards*
Creamware	All types recovered	1762–1820	1791	29	48
Delftware, Dutch/British	Painted, under free hand	1600–1802	1701	101	1
Pearlware	Undecorated	1775–1830	1802	27	6
Pearlware	Engine turned	1790–1830	1810	20	5
Pearlware	Painted, under free hand	1775–1820	1797	22	3
Porcelain, Chinese	Undecorated	1660–1860	1760	100	4
Porcelain, Chinese	Painted, over free hand	1660–1810	1735	75	7
Porcelain, Chinese	Painted, under free hand	1660–1860	1760	100	9
				Total	83
				MCD	1787

3–6% based upon inter-laboratory trials measuring low levels of water (< 500 ppm) in manufactured glasses (Geotti-Bianchini and De Riu 1995). We estimate a 1σ error at 4.5%. A 2σ error (9%) was used to calculate the margin of error associated with each date (Table 9). Improvements to the age estimate could be made in future applications by: (1) averaging a higher number of infrared scans (> 250) for each sample, and (2) averaging the means of multiple runs to tighten the probability distribution. This would help eliminate random error that may be caused by residual moisture present within the sample compartment.

The mean glass hydration date range (1771–93) is in very good agreement with the overall MCD of 1788 (Table 10). All of the date means are within the Monticello Phase II period or the beginning of Phase III. None of the mean age estimates are after the year 1800, when Jefferson covered the remains of Building o with clay fill as a result of extensive terracing of the hillside. Only two samples did not provide an adequate result. The fracture surface on sample DHR-304 was too thin to provide an adequate thermal response; and sample DHR-306 did not have a hydrated fracture, possibly because of recent breakage during excavation.

A careful look at the error range associated with each glass date is needed to assess the accuracy of the method. Not taking into account other potential sources of error such as ground temperature variation over time, the resolution of the absorbance measurements results in a 2σ error of 40–44 years. This is comparable in magnitude to standard deviations associated with many conventional radiocarbon dates. In comparison to the manufacturing ranges of ceramic types, the error is nearly twice as great compared to several forms of Pearlware, but much less than ceramic types such as freehand painted Chinese porcelain that was manufactured over several centuries. Thus, it appears that glass hydration may provide tighter chronological control for contexts containing pottery with long-term periods of manufacture, but it may be less useful in situations in which short-term ceramic forms are present.

CONCLUSION

The manufacturers of wine bottles from the early 17th century to the middle of the 19th century used a high-calcium, low-silica glass. Over an extended time period these glasses will develop a heavy surface patina as the bottles deteriorate. This process is especially noticeable on

archaeological specimens that have been in contact with ground water (Fig. 1). However, glass shards from non-saturated contexts do not have these surface layers, and this suggests that the glass structure is intact except for the inward diffusion of minute amounts of water. Under such circumstances, surface-water diffusion may be used to estimate the age of the artefact until structural deterioration begins.

We have conducted low-temperature (< 190°C) vapour hydration experiments on five compositionally different glasses to establish the Arrhenius constants. In hydration experiments at 80°C for 180 days, water diffusion in glass exhibited a square root of time dependence, but it rapidly accelerated at 210 days of exposure in all but one glass. SEM photographs of the surface revealed extensive cracking and disruption of the smooth surface. Only the glass with the highest silica content (DHR-145) remained intact and continued to show $t^{1/2}$ kinetics with 240 days of exposure to moisture.

SIMS profiles of the glasses added detail to this two-stage process. In the initial period of hydration, water diffusion was minimal. The hydrogen profile exhibited an error function shape and only the most minimal amount of sodium alkali exchange. In the longer exposures a double plateau hydrogen profile has been formed, with the simultaneous removal of sodium and potassium from the glass. Calcium is also highly mobile at the hydrogen diffusion front, but builds up near the glass surface. The same inter-diffusion of water and mobile ions is seen in an archaeological specimen, except that sodium and potassium are also significantly enriched at the surface of the glass. In the laboratory samples, we attribute this super-hydration to structural breakdown of the silica matrix as sodium and potassium are progressively removed. In the archaeological samples, the surface enrichment of the mobile species appears to form a surface layer that serves as a trap for ambient moisture.

To assess the compositional dependence of hydration, univariate and multivariate statistics were employed. Simple regressions revealed that the Arrhenius pre-exponential was poorly correlated with all of the glass major and minor constituents except for alumina. High-alumina glasses had lower pre-exponentials and higher activation energies, which are indicative of more durable glasses. Stepwise regression was then used to derive weighting factors that would estimate the pre-exponential and activation energy values based upon glass major components. SIMS analysis had revealed that CaO, K_2O and Na_2O were the mobile species that were involved in ion exchange and were probable predictor variables. The Arrhenius constant calibrations developed in this manner were used to calculate dates for archaeological glass fragments recovered from controlled excavations in Building o at Monticello. All of the dates fell within the expected date range documented through independent dating by historical ceramics and archival records.

These encouraging dating results should be tempered with a few cautionary statements. Methods that rely upon the measurement of external parameters such as soil temperature and relative humidity, and are subject to aggressive post-depositional processes, may not always provide results with integrity. For example, obsidian hydration dating tends to work best in environments in which the annual temperature and moisture extremes are low. Very arid environments should be avoided unless especially favourable conditions are present. In addition, highly alkaline soils may actually dissolve the developing hydration layer (Ambrose 1994) and artefacts within mobile sand deposits will be abraded (Stevenson *et al*. 1996). All of these limiting factors apply to the method developed here, and it is critical that the applicant of the method be familiar with site conditions and post-depositional processes. Glass shards from deep (e.g., 30 cm +) within archaeological deposits that are above the water table and not subject to alkaline attack or abrasion appear to be the most suitable contexts.

This application marks the first use of water diffusion in manufactured glasses to date an archaeological deposit. Although highly successful, these calibrations are preliminary and the experiment should be repeated with a much larger number of samples with greater compositional variability. The inward movement of water and counter diffusion of ions is a highly complex process to model even under simplified conditions in the laboratory. The archaeological SIMS profiles reveal that the archaeological inter-diffusion profile is different than the laboratory counterpart and that other variables have influenced the exchange process. We urge caution at this stage, but we see a great potential in this chronometric method to date the recent past.

ACKNOWLEDGEMENTS

We offer our sincere thanks to the Jeffress Memorial Trust, Richmond, Virginia, for funding this research. The Virginia Department of Historic Resources and the Thomas Jefferson Foundation were instrumental in providing opportunity and support, and for this we are very appreciative. Tom Devore, of the Department of Chemistry, James Madison University, provided very useful comments on a draft of the text. We also are grateful to Melba Meyers and Molly Gleeson for assistance in the laboratory. MDG and RJS acknowledge support from the National Science Foundation (Grant 0504015).

REFERENCES

Acocella, J., Tomozawa, M., and Watson, E. B., 1984, The nature of dissolved water in sodium silicate glasses and its effect on various properties, *Journal of Non-Crystalline Solids*, **65**, 355–72.

Adams, W. H., 2003, Dating historical sites: the importance of understanding time lag in the acquisition, curation, use and disposal of artifacts, *Historical Archaeology*, **37**(2), 38–64.

Ambrose, W., 1994, Obsidian hydration dating of a Pleistocene age site from the Manus Islands, Papua New Guinea, *Quaternary Geochronology*, **13**, 137–42.

Arrhenius, S., 1889, On the reaction velocity of the inversion of cane sugar by acids, *Zeitschrift für Physikalische Chemie*, **4**, 226.

Ashurst, D., 1970, Excavations at Gawber Glasshouse, near Barnsley, Yorkshire, *Post-Medieval Archaeology*, **4**, 92–140.

Binford, L., 1962, A new method of calculating dates from kaolin pipe stem samples, *Southeastern Archaeological Conference Newsletter*, **9**(1), 19–25.

Brill, R. H., 1999, *Chemical analyses of early glasses*, 2 vols, Corning Museum of Glass, Corning, New York.

Cable, M., and Smedley, J. W., 1987, Liquidus temperatures and melting characteristics of some early container glasses, *Glass Technology*, **28**(2), 94–8.

Crossley, D. W., and Arberg, F. A., 1972, Sixteenth-century glass-making in Yorkshire: excavations at furnaces at Hutton and Rosedale, North Riding, 1968–1971, *Post-Medieval Archaeology*, **6**, 107–59.

Cummings, K., Lanford, W. A., and Feldman, M., 1998, Weathering of glass in moist and polluted air, *Nuclear Instruments and Methods in Physics Research B*, **136–8**, 858–62.

DAACS, 2004, The Digital Archaeological Archive of Chesapeake Slavery (http://www.daacs.org/).

Dean, J., 1978, Independent dating in archaeological analysis, in *Advances in archaeological method and theory*, vol. 1 (ed. M. B. Schiffer), 223–55, Academic Press, New York.

Deetz, J., 1987, Harrington histograms versus Binford mean dates as a technique for establishing the occupational sequence of sites at Flowerdew Hundred, Virginia, *American Archaeology*, **6**(1), 62–7.

Doremus, R. H., 1975, Interdiffusion of hydrogen and alkali ions in a glass surface, *Journal of Non-Crystalline Solids*, **19**, 137–44.

Doremus, R. H., 2002, *Diffusion of reactive molecules in solids and melts*, John Wiley and Sons, Inc., New York.

Dungworth, D., 2005, *Investigation of 18th-century glass and glassworking waste from Lime-kiln Lane, Bristol*, Centre for Archaeology Report 7/2005, English Heritage, London.

El-Shamy, T. M., Morsi, S. E., Taki-Eldin, H. D., and Ahmed, A. A., 1975, Chemical durability of Na_2O–CaO–SiO_2 glasses in acid solutions, *Journal of Non-Crystalline Solids*, **19**, 241–50.

Friedman, I., and Long, W., 1976, Hydration rate of obsidian, *Science*, **19**, 347–52.

Friedman, I., Trembour, F. W., Smith, F. L., and Smith, G. I., 1994, Is obsidian dating affected by relative humidity? *Quaternary Research*, **41**, 185–90.

Geotti-Bianchini, F., and De Riu, L., 1995, Infrared spectroscopic analysis of water incorporated in the structure of industrial soda–lime–silicate glasses, *Glastechnische Berichte Glass Science and Technology*, **68**(7), 228–40.

Geotti-Bianchini, F., and Kramer, H. F., and Smith, I. H., 1999, Recommended procedure for the IR spectroscopic determination of water in soda–lime–silica glass, *Glastechnische Berichte Glass Science and Technology*, **72**(4), 103–11.

Glascock, M. D., 1998, Activation analysis. In *Instrumental multi-element chemical analysis* (ed. Z. B. Alfassi), 93–150, Kluwer Academic, Dordrecht.

Heighton, R. F., and Deagan, K. A., 1971, A new formula for dating kaolin clay pipestems, *The Conference on Historic Site Archaeology Papers*, **6**, 220–9.

Jackson, C. M., and Smedley, J. W., 2004, Medieval and post-medieval glass technology: melting characteristics of some glasses melted from vegetable and sand mixtures, *Glass Technology*, **45**(1), 36–42.

Kelso, W. M., 1986, Mulberry Row: slave life at Thomas Jefferson's Monticello, *Archaeology*, **39**(5), 28–35.

Kelso, W. M., 1997, *Archaeology at Monticello: artifacts of everyday life in the plantation community*, Monticello Monograph Series, Thomas Jefferson Foundation, Charlottesville, Virginia.

Kovel, R. M., and Kovel, T. H., 1953, *Dictionary of marks—pottery and porcelain*, Crown Publishers, New York.

Kovel, R. M., and Kovel, T. H., 1986, *Kovels' new dictionary of marks*, Crown Publishers, New York.

Lanford, W. A., 1977, Glass hydration: a method of dating glass objects, *Science*, **196**, 975–6.

Lanford, W. A., 1978, ^{15}N hydrogen profiling: scientific applications, *Nuclear Instruments and Methods*, **149**, 1–8.

Mazer, J. J., Stevenson, C. M., Ebert, W., and Bates, H., 1991, The experimental hydration of obsidian as a function of relative humidity and temperature, *American Antiquity*, **56**, 504–13.

Melcher, M., and Schreiner, M., 2005, Evaluation procedure for leaching studies on naturally weathered potash–lime–silica glasses with medieval composition by scanning electron microscopy, *Journal of Non-Crystalline Solids*, **351**, 1210–25.

Miller, G., 2000, Telling time for the archaeologist, *Northeast Historical Archaeology*, **29**, 1–22.

Noel Hume, I., 1970, *A guide to the artifacts of Colonial America*, Alfred A. Knopf, New York; originally published in 1969.

Romich, H., 2003, Studies of ancient glass and their application to nuclear-waste management, *Materials Research Society Bulletin*, July, 500–4.

Sinton, C. W., and LaCourse, W. C., 2001, Experimental survey of the chemical durability of commercial soda–lime–silicate glasses, *Materials Research Bulletin*, **36**, 2471–9.

Smets, B. M. J., and Lommen, T. P. A., 1983, The role of molecular water in the leaching of glass, *Physics and Chemistry of Glasses*, **24**(1), 35–6.

South, S., 1972, Evolution and horizon as revealed in ceramic analysis in historical archaeology, *Conference on Historic Site Archaeology Papers*, **6**, 71–116.

Speakman, R. J., and Neff, H. (eds.), 2005, *Laser ablation ICP–MS in archaeological research*, University of New Mexico Press, Albuquerque.

Stevenson, C. M., Mazer, J. J., and Scheetz, B. E., 1998, Laboratory obsidian hydration rates: theory, method and application, In *Archaeological obsidian studies: method and theory* (ed. S. Shackley), 181–204, Advances in Archaeological and Museum Science, vol. 3, Plenum Press, New York.

Stevenson, C. M., Sheppard, P. J., Sutton, D. G., and Ambrose, W., 1996, Advances in the hydration dating of New Zealand obsidian, *Journal of Archaeological Science*, **23**, 233–42.

Trembour, F. W., Smith, F. L., and Friedman, I., 1988, Diffusion cells for integrating temperature and humidity over long periods of time, *Materials Research Society Symposium Proceedings*, **123**, 245–51.

Turner, W. E. S., 1956, Studies in ancient glasses and glassmaking processes, part V; raw materials and melting processes, *Journal of the Society of Glass Technology*, **40**, 277–300.

Wassick, T. A., Doremus, R. H., Lanford, W. A., and Burman, C., 1983, Hydration of soda–lime silicate glass, effects of alumina, *Journal of Non-Crystalline Solids*, **54**, 139–51.

Wilcoxen, C., 1987, *Dutch trade and ceramics in America in the seventeenth century*, Albany Institute of History and Art, Albany.